Study of the H+HS reaction on a newly built potential energy surface using the quasi-classical trajectory method*

Bai Meng-Meng(白孟孟), Ge Mei-Hua(葛美华), Yang Huan(杨 欢)†, and Zheng Yu-Jun(郑雨军)

School of Physics, Shandong University, Jinan 250100, *China*

(Received 16 April 2012; revised manuscript received 9 May 2012)

The quasi-classical trajectory (QCT) method is used to study the H+HS reaction on a newly built potential energy surface (PES) of the triplet state of H_2S ($^3A''$) in a collision energy range of 0–60 kcal/mol. Both scalar properties, such as the reaction probability and the integral cross section (ICS), and the vector properties, such as the angular distribution between the relative velocity vector of the reactant and that of the product, etc., are investigated using the QCT method. It is found that the ICSs obtained by the QCT method and the quantum mechanical (QM) method accord well with each other. In addition, the distribution for the product vibrational states is cold, while that for the product rotational states is hot for both reaction channels in the whole energy range studied here.

Keywords: quasi-classical trajectory, integral cross section, scalar properties, vector properties

PACS: 34.50.–s, 34.50.Lf, 31.15.xv, 31.15.ap **DOI:** 10.1088/1674-1056/21/12/123401

1. Introduction

Nowadays, more and more groups are using the rigorous quantum mechanical (QM) method to study the reaction dynamics for the elementary reactions in gas phase, and so far the systems have been extended from three atoms to four atoms.[1−5] However, it is not so easy because the computational cost will be squared as the number of atoms increases from 3 to 4. And even for the three-atom system, it is extremely time-consuming to acquire the information about the integral cross sections (ICSs) or the rate constants, as the reaction probabilities for all total angular momenta J_s that are converged to a certain energy are needed.[6−10] Fortunately, the quasi-classical trajectory (QCT) method could serve as a substitution to obtain these quantities. With the help of the QCT method, less computational cost is needed, but relatively good results for statistical quantities, such as the ICSs, the rate constants and so on, could be obtained.[11−13] Hence despite the existence of the rigorous QM method, the QCT method is still robust to be used for studying the isotope effect,[14] the influence of reagent ro-vibrational excitation,[15,16] and the effect of collision energy[17] on stereodynamics.

The H+H′S→HH′+S/HS+H′ reaction is one of the simplest reactions that involve sulfur atoms and provides the prototype for studying the hydrogen-atom abstraction and exchange reactions. The reactants H(^{2}S)+HS($^2\Pi$) correlate to both the singlet state of H_2S ($^1A'$ and $^1A''$) and the triplet state of H_2S ($^3A'$ and $^3A''$). The $^3A''$ state is the lowest adiabatic triplet state of H_2S, and the H+HS reaction can proceed through competitive H-abstraction and H-exchange pathways in this state. The first potential energy surface (PES) for H_2S ($^3A''$) was created by Maiti *et al.*[18] for the purpose of studying the importance of intersystem crossing in the S(^{1}D, ^{3}P)+H_2 reaction. Then, Klos *et al.*[19] built an analytical PES for H_2S ($^3A''$) according to the multi-reference configuration interaction (MRCI) method with AVQZ basis set. Recently, Lü *et al.*[20] constructed a new high-quality PES for this triplet state in light of MRCI method with AV5Z basis set. They also presented the results of ICSs from QM calculations. In view of few reaction dynamical studies are conducted on the triplet $^3A''$ state for the H+HS reaction, we investigate this reaction in the triplet $^3A''$ state using the

*Project supported by the National Natural Science Foundation of China (Grant No. 21073110), the Independent Innovation Foundation of Shandong University, China (Grant No. 2010GN030), and the National Science Foundation for Postdoctoral Scientists of China (Grant No. 20100481280).

†Corresponding author. E-mail: h.yang@sdu.edu.cn

© 2012 Chinese Physical Society and IOP Publishing Ltd

QCT method for verifying the QCT method and acquiring other information about the reaction dynamics.

The PES used in the calculation is the newly built PES by Lü *et al.*[20] There are no wells for both reaction channels and the minimum energy paths (MEPs) of the abstraction and exchange processes occurring at the collinear configurations. So the barrier heights increase when S–H–H and H–S–H bond angles decrease from 180°. The barrier heights for linear S–H–H and H–S–H are 2.07 kcal/mol and 7.15 kcal/mol, respectively. Figure 1 shows the schematic diagram along the MEPs for both reaction channels. The values in parentheses are the values of corresponding zero-point energy (ZPE) and all energies are given in units of kcal/mol with respect to the reactant H+HS asymptote.

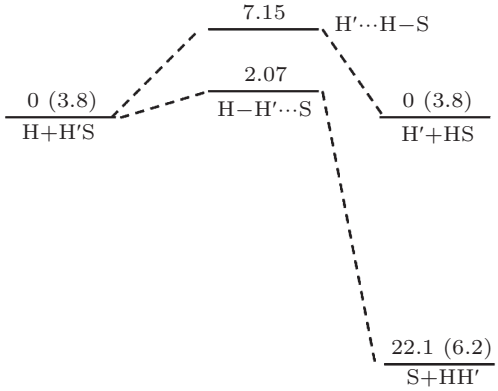


Fig. 1. Schematic diagram of the barriers and transition states along the minimum energy path for both reaction channels on the $^3A''$ electronic state. Values in parentheses are the corresponding zero-point energies. All energies are valued with respect to the reactant H+HS asymptote and are given in units of kcal/mol.

The rest of the present paper is organized as follows. In Section 2, the computational details, especially the key parameters used in the calculation, are described. The results and discussion about the scalar properties and the vector properties are presented in Section 3. The conclusions are drawn from the present study in Section 4.

2. Computational details

The method used here is the QCT method. This method has been widely described in Refs. [21]–[27], hence no more descriptions will be given here, apart from a brief description of some key parameters that are relevant to the calculation. First, the radius of collision (ρ), which is used to determine the bond breaking or forming of the diatoms, is 10 angstroms; then the time step size used to do the iterations is 1 fs. One of the most important parameters for the QCT calculations is the maximum impact parameter ($b_{\max}$), which can be used to obtain the ICS according to

$$\sigma = \pi b_{\max}^2 \frac{N_{\rm r}}{N_{\rm t}}, \tag{1}$$

where $N_{\rm r}$ is the number of trajectories that go into a certain reaction channel and $N_{\rm t}$ is the total number of trajectories. It should be mentioned that there is the correspondence among $b_{\max}$ and each pair of collision energy (in units of kcal/mol in this paper) and reaction channel. And $b_{\max}$ could be picked out following the rules that no more reactions would happen in one reaction channel at a certain collision energy. All $b_{\max}$s for different collision energies in both reaction channels are listed in Tables 1 and 2. Last but not the least, batches of 10000 trajectories were run for each calculation. In this study, all initial states of reactants were kept in their ground ro-vibrational states, and effects of ro-vibrational excitations on the reaction dynamics will be studied in the future.

Table 1. Values of $b_{\max}$ (Å) for different collision energies (kcal/mol) in the H+HS→H_2+S reaction channel.

E	2	3	6	9	12	15	18	21	24	27	30	33	36	39	42	45
$b_{\max}$	0.85	1.63	2.62	2.70	2.67	2.74	2.73	2.72	2.70	2.75	2.74	2.72	2.73	2.67	2.74	2.73

Table 2. Values of $b_{\max}$ for different collision energies in the H+H′S→HS+H′ reaction channel (Units are the same as those in Table 1).

E	6	9	12	15	18	21	24	27	30	33	36	39	42	45
$b_{\max}$	0.37	0.96	1.17	1.27	1.37	1.39	1.43	1.48	1.48	1.48	1.50	1.50	1.52	1.54

3. Results and discussion

Figure 2 shows the reaction probabilities and ICSs versus collision energy (in units of kcal/mol) for the H_2+S and HS+H product channels, respectively. It can be seen from Fig. 2(a) that the two curves present different features. The black-solid-circle line represents the reaction probability for the exchange channel. There is a threshold for this channel, which is around 6 kcal/mol according to the figure, and the reaction probability increases almost monotonically with collision energy increasing. While for the other channel, which is represented with red-solid-square line, in this abstraction channel the reaction can occur with almost no collision energy (the threshold lies around 2 kcal/mol). However at the beginning the probability is so small that it can be neglected, then it varies slightly around 0.06 once the collision energy exceeds 9 kcal/mol. In addition, the reaction probability for the exchange channel is larger than that for the abstraction channel when the collision energy is over 9 kcal/mol.

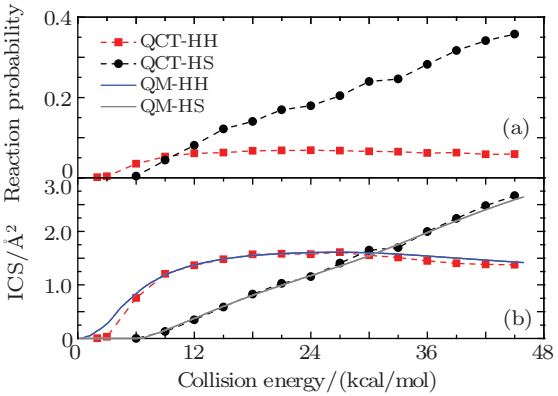


Fig. 2. (color online) Reaction probabilities and ICSs versus collision energy for both product channels. The curves with black solid circles and red solid squares are obtained from the QCT calculations, while those gray solid and blue solid lines are obtained from rigorous quantum mechanical calculations in Ref. [20].

Figure 2(b) shows the ICSs for both product arrangement channels, and also show the results from the rigorous QM calculations in Ref. [20]. The two results for the HS+H product channel fit to each other very well, not only for the threshold energy but also for the magnitude. Though they differ a little from the abstraction reaction channel mainly in the high energy region and in extremely low energy regions, the conclusion that quantum effects have little influence on the reaction probability[20] still works for the QCT results, which is result from the feature of the PES. As no wells exist along the MEPs, the reactions are dominated by the barriers of the transition states. The difference in threshold between the QM and QCT methods is due to a well-known handicap of classical mechanics as zero-point energy (ZPE) leakage.[28] When collision energy goes beyond 30 kcal/mol, the ICSs for the exchange channel begin to exceed the ICSs for the abstraction channel. The turning points for the ICSs and reaction probabilities are not the same, as the behaviours of ICSs are determined by two factors, the reaction probability and the max impact parameter, according to Eq. (1). The abstraction channel dominates at low collision energy, while the exchange channel becomes dominant immediately after the energy has exceeded the barrier of the exchange reaction. It could be explained as the point that the exchange reaction has a larger acceptance cone than the abstraction reaction for the two competitive channels.

From the comparisons between results obtained by the QCT method and the expensive QM method, it could be easily seen that the QCT method works as well as the QM method when treating statistical quantities, such as ICSs, on this PES. So it gives us confidence to show other statistical results obtained by the QCT method in the following.

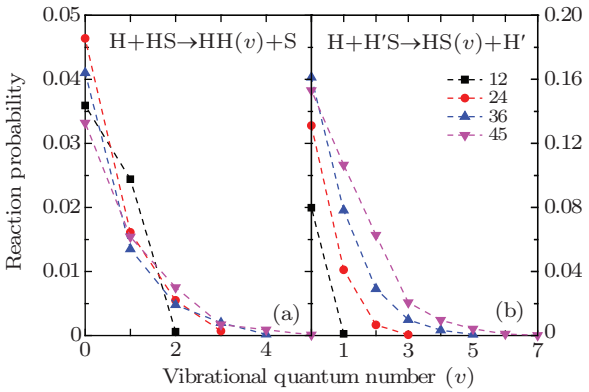


Fig. 3. (color online) Product vibrational quantum state distributions for the abstraction and exchange channels at 12, 24, 36, and 45 kcal/mol.

Figure 3 shows the product vibrational quantum state distributions for both product arrangement channels at four separated collision energies, 12, 24, 36, and 45 kcal/mol. The two panels exhibit the same behaviours, that is, the distributions of vibrational quantum states are not inverted and more vibrational channels of products are open as the collision energy increases. But there are differences between the two panels. The probability for the HS+H channel is larger than that for the H_2+S channel, and more

vibrational quantum states are accessible for the exchange channel under the same condition of collision energy. It is consistent with the fact the HS+H product channel is dominated in reaction probability when energy is above 9 kcal/mol, which can be seen from Fig. 2(a).

Figure 4 shows the product rotational quantum state distributions for the two reaction channels at five different collision energies, 9, 18, 27, 36, and 45 kcal/mol. In contrast to the distributions of vibrational states, the distributions for the rotational states are hot and as the energy increases the most pronounced states shift toward the higher rotational quantum states. Similar to the case of vibrational state distribution, the exchange channel is more preferred and more rotational quantum states are open at the same collision energy. But there is an obvious distinction between the two figures, that is, the amplitudes of peaks go smaller for the H_2+S product channel, while they become larger for the HS+H product channel when the collision energy varies from 9 kcal/mol to 45 kcal/mol. It could be explained as follows: when energy grows the rotational excited HS products are more easily to produce, but the reactions that produce rotational excited H_2 are restricted.

So far, parts of scalar properties about the reaction dynamics have been presented. Thanks to the stereodynamics QCT method, some of the vector properties, such as the $\boldsymbol{k}$ (the relative velocity vector of the reactant)–$\boldsymbol{k}'$ (the relative velocity vector of the product) angular distributions $\mathrm{P}(\theta_\mathrm{t})$, the $\boldsymbol{k}$–$\boldsymbol{j}'$ (the rotational angular momentum of the product) angular distributions $\mathrm{P}(\theta_\mathrm{r})$, $\boldsymbol{k}$–$\boldsymbol{k}'$–$\boldsymbol{j}'$ correlations $\mathrm{P}(\varphi_\mathrm{r})$, and so on could also be brought to light. The usual space-fixed right-handed coordinate system is employed in the QCT calculation, which has its origin placed at the centre of the mass of the reagent diatomic molecule, the attacking atom placed in the YZ plane initially, the relative velocity vector $\boldsymbol{k}$ pointing along the positive direction of the Z axis, and the XZ plane containing both $\boldsymbol{k}$ and $\boldsymbol{k}'$ vectors. The θ_r and φ_r are the azimuthal angle of the rotational angular momentum j' and the dihedral angle between the $\boldsymbol{k}$–$\boldsymbol{k}'$ and $\boldsymbol{k}$–$\boldsymbol{j}'$ planes, respectively. Details about these correlations and expressions of these distributions have been repeated many times in the literature,[29–35] so readers are referred to these references for more details.

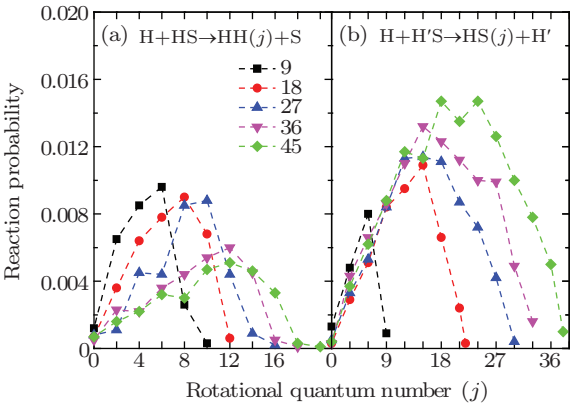


Fig. 4. (color online) The product rotational quantum state distributions for the H_2+S product channel and for the HS+H product channel at 9, 18, 27, 36, and 45 kcal/mol.

Figure 5 shows the curves for $\boldsymbol{k}$–$\boldsymbol{k}'$ correlation $\mathrm{P}(\theta_\mathrm{t})$ for both product arrangement channels. The $\mathrm{P}(\theta_\mathrm{t})$ is known as the differential cross section (DCS), where θ_t is the scattering angle between the initial and final relative velocity vectors. The 0°∼180° angular range of θ_t is divided into 20 bins and the value of cross section per solid angle $(\mathrm{d}\sigma/\mathrm{d}\Omega)$ is specified at the central point of the interval,

$$\mathrm{P}(\theta_\mathrm{t}) = \frac{\mathrm{d}\sigma}{\mathrm{d}\Omega} = \pi b_{\max}^2 \frac{N_\mathrm{r}(\theta_\mathrm{t})}{N_\mathrm{t}} \times \frac{1}{2\pi \sin\theta_\mathrm{t}}, \qquad (2)$$

where $N_\mathrm{r}(\theta_\mathrm{t})$ is the number of trajectories going into the θ_t interval for a certain specified product channel. For the exchange channel, the distributions are obviously backward for the energy range considered here, but there is a trend that the distribution shifts slightly to a forward scattering angle; while for the abstraction channel, the distribution is predominately backward for the lowest collision energy (12 kcal/mol), but as energy increases the distribution becomes symmetrical (24 kcal/mol) and at higher energy values the forward scattering clearly dominates (36 kcal/mol and 45 kcal/mol). It is not difficult to understand the asymmetrical feature of $\mathrm{P}(\theta_\mathrm{t})$ distribution, as there are no wells but only barriers along the reaction paths for both channels. So no long-lived complexes will be generated and the scattering will be anisotropic. The differences in $\mathrm{P}(\theta_\mathrm{t})$ distribution between the two channels result from the distinct mass ratios of product fragments and from the different features of the PES. The influence of collision energy on the $\boldsymbol{k}$–$\boldsymbol{k}'$ correlation could be explained on the basis of impulsive effect, that is, the effect that more repulsive parts of the PES are energetically accessible as energy in-

creases cannot counterbalance it.[36]

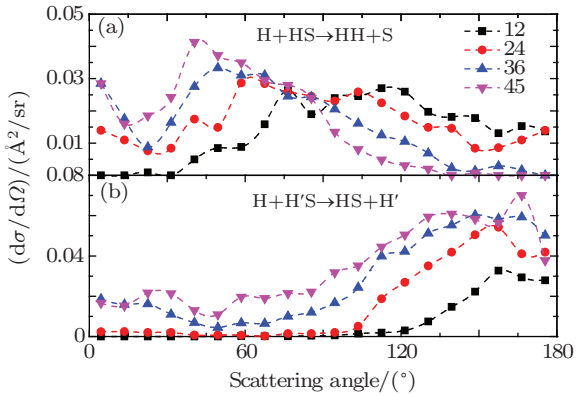


Fig. 5. (color online) $\boldsymbol{k}$–$\boldsymbol{k}'$ angular distributions expressed in terms of cross section per solid angle for both reaction channels at four collision energies, 12, 24, 36, and 45 kcal/mol.

Figure 6 shows the curves of $\boldsymbol{k}$–$\boldsymbol{j}'$ angular correlation $P(\theta_r)$ for both product arrangement channels, which can be used to extract the alignment information about the rotational angular momentum vector $\boldsymbol{j}'$ for the product relative to the $\boldsymbol{k}$ direction. The $\boldsymbol{k}$–$\boldsymbol{j}'$ angular correlations are symmetrical around 90° for all collision energies and for both reaction channels, which reveals that the directions of the rotational angular momentum $\boldsymbol{j}'$ for the products are mainly perpendicular to the directions of the relative velocity $\boldsymbol{k}$ for the reactants. However, it is not enough to determine the direction of $\boldsymbol{j}'$ only with the $P(\theta_r)$ distribution, so we need to combine with the $\boldsymbol{k}$–$\boldsymbol{k}'$–$\boldsymbol{j}'$ correlation $P(\phi_r)$, which is represented in Fig. 7. It is clear that the direction of $\boldsymbol{j}'$ orientates along the negative Y axis. The influences of collision energy on $\boldsymbol{k}$–$\boldsymbol{j}'$ and $\boldsymbol{k}$–$\boldsymbol{k}'$–$\boldsymbol{j}'$ correlations can be explained by the chemical reactivities of the two competitive channels.

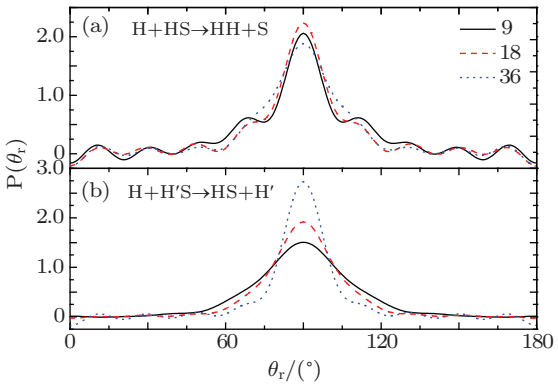


Fig. 6. (color online) Curves of $\boldsymbol{k}$–$\boldsymbol{j}'$ angular distribution $P(\theta_r)$ for both reaction channels at three collision energies, 9, 18, and 36 kcal/mol.

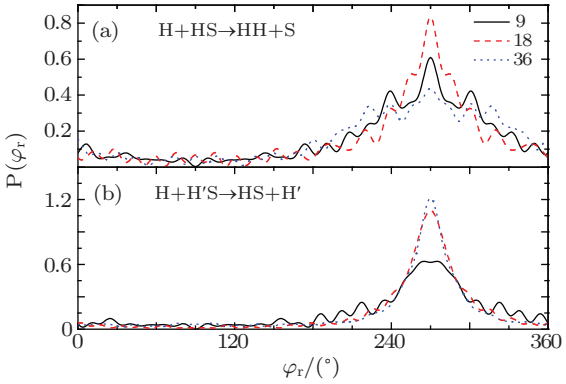


Fig. 7. (color online) Curves of $\boldsymbol{k}$–$\boldsymbol{k}'$–$\boldsymbol{j}'$ angular distribution $P(\phi_r)$ for both reaction channels at three collision energies, 9, 18, and 36 kcal/mol.

4. Conclusion

We studied the reaction dynamics for the H+HS ($v = 0$, $j = 0$) →H_2+S/HS+H reaction employing the newly built H_2S ($3A''$) PES. Both the scalar properties and the vector properties were investigated by using the QCT method. The comparisons between the results obtained from the QCT method and the QM method show obviously that the QCT method holds true for treating statistical quantities for the title reaction. The $\boldsymbol{k}$–$\boldsymbol{k}'$ correlations are basically asymmetric, which indicates there exist no long-lived complexes, and the direction of rotational angular momentum $\boldsymbol{j}'$ for the product is mainly perpendicular to the direction of the relative velocity $\boldsymbol{k}$ for the reactant.

References

[1] Lu R F, Zhang P Y, Chu T S, Xie T X and Han K L 2007 *J. Chem. Phys.* **126** 124304
[2] Valero R, McCormack D A and Kroes G J 2004 *J. Chem. Phys.* **120** 4263
[3] Medvedev D M, Gray S K, Goldfield E M, Lakin M J, Troya D and Schatz G C 2004 *J. Chem. Phys.* **120** 1231
[4] Liu S, Xu X and Zhang D H 2011 *J. Chem. Phys.* **135** 141108
[5] Song H W, Lu Y P and Lee S Y 2011 *J. Chem. Phys.* **135** 014305
[6] Chu T S, Zhang Y and Han K L 2006 *Int. Rev. Phys. Chem.* **25** 201
[7] Xie T X, Zhang Y, Zhao M Y and Han K L 2003 *Phys. Chem. Chem. Phys.* **5** 2034
[8] Chu T S and Han K L 2008 *Phys. Chem. Chem. Phys.* **10** 2431
[9] Chu T S and Han K L 2005 *J. Phys. Chem.* A **109** 2050
[10] Yang H, Han K L, Schatz G C, Lee S H, Liu K, Smith S C and Hankel M 2009 *Phys. Chem. Chem. Phys.* **11** 11587
[11] Jorfi M and Honvault P 2011 *Phys. Chem. Chem. Phys.* **13** 8414

[12] Han B R, Yang H, Zheng Y J and Varandas A J C 2010 *Chem. Phys. Lett.* **493** 225
[13] Liang J J, Yang C L, Wang L Z and Zhang Q G 2012 *Chem. Phys.* **392** 180
[14] Xiao J, Yang C L and Wang M S 2012 *Chin. Phys.* B **21** 043101
[15] Li S J, Shi Y, Xie T X and Jin M X 2012 *Chin. Phys.* B **21** 013401
[16] Zhao J and Luo Y 2011 *Chin. Phys.* B **20** 043402
[17] Yu Y J, Xu Q and Xu X W 2011 *Chin. Phys.* B **20** 123402
[18] Maiti B, Schatz G C and Lendvay G 2004 *J. Phys. Chem.* A **108** 8772
[19] Klos J A, Dagdigian P J and Alexander M H 2007 *J. Chem. Phys.* **127** 10
[20] Lü S J, Zhang P Y, Han K L and He G Z 2012 *J. Chem. Phys.* **136** 094308
[21] Han K L, He G Z and Lou N Q 1996 *J. Chem. Phys.* **105** 8699
[22] Han K L, He G Z and Lou N Q 1993 *Chin. Chem. Lett.* **4** 517
[23] Li R J, Han K L, Li F E, Lü R C, He G Z and Lou N Q 1994 *Chem. Phys. Lett.* **220** 281
[24] Liu S L and Shi Y 2010 *Chin. Phys. Lett.* **27** 123103
[25] Wang T and Yue X F 2011 *Chin. Phys. Lett.* **28** 023101
[26] Ge M H and Zheng Y J 2011 *Theor. Chem. Acc.* **129** 173
[27] Ge M H and Zheng Y J 2011 *Chem. Phys.* **129** 185
[28] Varandas A J C 1993 *J. Chem. Phys.* **99** 1076
[29] Kang L H and Zhu M Y 2010 *J. Mol. Struc. Theochem* **945** 116
[30] Xu W W, Liu X G, Luan S X and Mang Q G 2010 *Int. J. Quantum Chem.* **110** 860
[31] Chen T Y, Zhao N J, Zhang W P and Wang X Q 2011 *Cent. Eur. J. Phys.* **9** 1221
[32] Wu V W K 2011 *Phys. Chem. Chem. Phys.* **13** 9407
[33] Xu Z and Zong F J 2010 *J. Mol. Struc. Theochem* **960** 22
[34] Aoiz F J, Brouard M, Herrero V J, Rabanos V S and Stark K 1996 *Chem. Phys. Lett.* **264** 487
[35] Ge M H and Zheng Y J 2011 *Chin. Phys.* B **20** 083401
[36] Gonzlez M, Sierra J D, Francia R and Says R 1997 *J. Phys. Chem.* A **101** 7513